Anal. Chem. **2002,** *74,* 5913−5918

Articles

A Disposable, Reagentless, Third-Generation Glucose Biosensor Based on Overoxidized Poly(pyrrole)/Tetrathiafulvalene−Tetracyanoquinodimethane Composite

Francesco Palmisano* and Pier Giorgio Zambonin

Dipartimento di Chimica, Università di Bari, Via Orabona, 4-70126 Bari, Italy

Diego Centonze and Maurizio Quinto

Istituto di Preparazioni e Produzioni Alimentari, Facoltà di Agraria, Università di Foggia, Via Napoli, 25-71100 Foggia, Italy

A disposable glucose biosensor based on glucose oxidase immobilized on tetrathiafulvalene−tetracyanoquinodimethane (TTF−TCNQ) conducting organic salt synthesized in situ onto an overoxidized poly(pyrrole) (PPy_{ox}) film is described. The TTF−TCNQ crystals grow through the nonconducting polypyrrole film (ensuring electrical connection to the underlying Pt electrode) and emerge from the film forming a treelike structure. The PPy_{ox} film prevents the interfering substances from reaching the electrode surface. The sensor behavior can be modeled by assuming a direct reoxidation of the enzyme at the surface of the TTF−TCNQ crystals. A heterogeneous rate constant around $10^{-6}-10^{-7}$ cm s^{-1} has been estimated. The biosensor is nearly oxygen- and interference-free and when integrated in a flow injection system displays a remarkable sensitivity (70 nA/mM) and stability.

In the course of the past decade, great efforts have been devoted toward the characterization of a large variety of amperometric enzyme biosensors for clinical, environmental, and food analysis. Since, for most redox enzymes, direct electron transfer is a very inefficient process,[1−3] mediated electrochemistry is typically used. When the electron acceptor is the natural mediator (first-generation biosensors), an obvious limitation is the dependence of the sensor response on the mediator (e.g., oxygen) concentration. To solve this problem, second-generation biosensors based on artificial mediators[4−14] have been introduced. The mediator can be retained at the electrode surface by a discrete membrane, mixed with the enzyme in a carbon paste or entrapped in an electrogenerated film.[13,15] However, leaching of the mediator from the electrode surface rapidly deteriorates the biosensor response.[12−14] Alternatively, the mediator can be covalently attached to the polymer incorporating the enzyme[10] or to the immobilized enzyme itself.[11]

Conducting organic salt[16−18] (COS)-based electrodes appear potentially able to solve the above-mentioned problems. COS, such

* Corresponding author. Phone: +39-080-5442016. Fax: +39-080-5442026. E-mail: palmisano@chimica.uniba.it.

(1) Dryhurst, G.; Kadish, K. M.; Scheller, F.; Renneberg, R. *Biological Electrochemistry;* Academic Press: New York, 1982; Vol. 1, p 398.
(2) Degani, Y.; Heller, A. *J. Am. Chem. Soc.* **1989**, *111*, 2357.
(3) Ghindilis, A. L.,; Atanasov, P.; Wilkins, E. *Electroanalysis* **1997**, *9*, 661.
(4) Cass, A. E. G.; Davis, G.; Francis, G. D.; Hill, H. A. O.; Aston, W. J.; Higgins, I. J.; Plotkin, E. V.; Scott, L. D. L.; Turner, A. P. F. *Anal. Chem.* **1984**, *56*, 667.
(5) Ianniello, R. M.; Lindsay, T. J.; Yacynych, A. M. *Anal. Chem.* **1982**, *54*, 1980.
(6) Lauge, M. A.; Chambers, J. Q. *Anal. Chim. Acta* **1985**, *175*, 89.
(7) Kulys, J. J.; Cenas, N. K. *Biochim. Biophys. Acta* **1983**, *744*, 57.
(8) Ikeda, T.; Hamada, H.; Miki, K.; Senda, M. *Agric. Biol. Chem.* **1985**, *49*, 541.
(9) Umana, M.; Waller, J. *Anal. Chem.* **1986**, *58*, 2979.
(10) Hale, P. D.; Inagaki, T.; Karan, H. I.; Okamoto, Y.; Skothein, T. A. *J. Am. Chem. Soc.* **1989**, *111*, 3482.
(11) Degani, Y.; Heller, A. *J. Phys. Chem.* **1987**, *91*, 1285.
(12) Yokoyama, K.; Tomiya, E.; Karube, I. *Anal. Lett.* **1989**, *22*, 2949.
(13) Foulds, N. C.; Lowe, C. R. *Anal. Chem.* **1988**, *60*, 2473.
(14) Kajiya, Y.; Sugai, H.; Iwakura, C.; Yoneyama, H. *Anal. Chem.* **1991**, *63*, 49.
(15) Du, G.; Lin, C.; Bocarsly, A. B. *Anal. Chem.* **1996**, *68*, 796.
(16) Cenas, N. K.; Kulys, J. J. *Bioelectrochem. Bioenerg.* **1981**, *8*, 103.
(17) Albery, W. J.; Bartlett, P. N.; Craston, D. H. *J. Electroanal. Chem.* **1985**, *194*, 223.
(18) Albery, W. J.; Bartlett, P. N. *J. Electroanal. Chem.* **1985**, *194*, 223,

10.1021/ac0258608 CCC: $22.00
Published on Web 10/31/2002

as tetrathiafulvalene−tetracyanoquinodimethane (TTF−TCNQ), are known to mediate the electrochemistry of pyrrole−quinoline-quinone enzymes[19,20] (e.g., PQQ-dehydrogenase), as well as of flavoproteins[17,18,21] (e.g., glucose oxidase, GOx). Different electron-transfer mechanisms (homogeneous mediation,[7] heterogeneous catalysis,[17] direct electron transfer[22]) have been proposed by different authors, but the matter still remains controversial.

COS-based biosensors are typically constructed using either polymer-bound, pressed pellets or sublimed polycrystalline electrodes, with enzymes immobilized by glutaraldehyde (glut) cross-linking,[23−26] adsorption,[27] and discrete membranes,[17,18,21] including electrogenerated films.[28,29] Disposable COS-based biosensors cannot be easily produced, and only few attempts have been reported so far. Khan et al.[30] described a glucose sensor based on GOx/TTF−TCNQ binder paste that could be manually applied on a conventional cavity-type electrode; alternatively, the paste could be applied on a Pt-coated working electrode of a sensor chip through a specially designed screen having a hole of 2-mm diameter in order to obtain a recessed cavity.

However, the described approach, where the COS preparation followed the classical procedure, did not allow the fabrication of a truly disposable biosensor, e.g., a device having a complete three-electrode system in a single planar chip.

In the present work, the fabrication of a reagentless disposable glucose biosensor based on TTF−TCNQ is described. A new and relatively simple procedure has been devised, consisting of a sequential casting of the individual reagents (TTF, TCNQ, BSA−glut−GOx) onto a nonconducting polypyrrole-modified Pt working electrode of a low-cost three-electrode disposable chip. The biosensor has been characterized in terms of electrode mechanism, stability, linearity, oxygen dependence, and interference rejection.

EXPERIMENTAL SECTION

Chemicals. Glucose oxidase (type VII from *Aspergillus niger*, 168.000 units/g), β-D-glucose, tetrathiafulvalene, tetracyanoquinodimethane, glutaraldehyde (grade II, 25% aqueous solution), ascorbic acid, acetaminophen, uric acid, and L-cysteine (Sigma Chemical Co., St. Louis, MO) were used as received. Glucose stock solutions were prepared in phosphate buffer (pH 7.0, I = 0.1) and left at 4°C overnight to allow the equilibration of the anomers. Pyrrole (Aldrich, Steinheim, Germany) was purified before use by vacuum distillation at 65 °C, and stored at −28 °C under nitrogen atmosphere. All the other chemicals were of analytical grade. Phosphate buffer (pH 7.0, I = 0.1) was used as the carrier in flow injection experiments.

Apparatus. All the electropolymerization experiments were carried out with a PAR 263 A (EG&G, Princeton Applied Research, Princeton, NJ) controlled by a computer. All the other electrochemical experiments were performed by a PAR EC 400 electrochemical detector, coupled with an in-house-built data acquisition system whose acquisition software was written in Microsoft QuickBasic.

The screen-printed electrodes (Ing. Krejci Engineering, Tisnov, Slovak Republic) consisted of a platinum working electrode, surrounded by a quasi-reference electrode (Ag/AgCl paste), and a Pt counter electrode, which is the outermost ring of the device. The working electrode had an active area of (0.43 ± 0.03) mm^2 determined, on 10 different devices, by means of linear scan voltammetry, in a ferrocyanide solution.[31] All batch measurements were performed in a stirred phosphate buffer solution (PBS, pH 7.0) containing 10 mM Cl^-. In this way, a stable potential for the reference electrode could be obtained. Flow injection experiments were performed by using a Gilson (Gilson Medical Electronics) Minipuls 3 peristaltic pump and a six-way low-pressure injection valve (Rheodyne, Cotati, CA). Biosensors were inserted in a homemade Plexiglas flow-through cell (dimensions: 27 × 42 × 14 mm^3). The volume of the flow cell, assembled with a 0.2-mm-thick gasket, was 120 μL.

Preparation of Enzyme Electrodes. The PPy films were electrochemically grown at +0.7 V versus Ag/AgCl in a deoxygenated 10 mmol L^{-1} KCl solution containing 0.4 mol L^{-1} pyrrole. Unless otherwise specified, the deposition charge was 800 mC/cm^2 since, as already shown,[32] this value gives the best anti-interference properties. The PPy film (estimated thickness 0.6−1.0 μm) was then overoxidized overnight at 0.7 V versus Ag/AgCl in PBS (I = 0.1, pH 7.0).

The TTF−TCNQ layer was prepared by a two sequential steps procedure. In the first step, 1 μL of a TCNQ solution (in THF) was cast on the PPy_{ox} layer and left for a few minutes on the laboratory bench to complete drying. In the second step, 1 μL of saturated solution of TTF in acetonitrile (containing an excess amount of TTF over TCNQ) was slowly spread over the TCNQ-cast PPy_{ox} film and kept in a relatively cool place. The complete casting procedure (both TCNQ and TTF steps) was repeated in order to ensure complete surface coverage. After several minutes, when the film became completely dry and the crystallization of TTF−TCNQ was completed, the electrode was gently washed with acetonitrile and finally with diethyl ether until the yellow color of the unreacted TTF was completely removed. The Pt/PPy_{ox}/TTF−TCNQ electrode was modified by a GOx-containing gel prepared as follows. Two hundred microliters of PBS (I = 0.1, pH 6.8), containing 7 mg of BSA and 2 mg of GOx, was carefully mixed with 20 μL of a 2.5% glutaraldehyde solution. A 2-μL sample of the mixture was then pipetted onto the working electrode surface and air-dried at room temperature. Sensors were thoroughly washed after preparation and, when not in use, stored in a phosphate buffer (I = 0.1, pH 7.0) at 4 °C.

(19) D'Costa, E. J.; Higgins, I. J.; Turner, A. P. F. *Biosens. Bioelectron.* **1986**, *2*, 71.
(20) Zhao, S.; Lennox, R. B. *Anal. Chem.* **1991**, *63*, 1174
(21) Sekine, Y.; Hall, E. A. H. *Biosens. Bioelectron.* **1998**, *13*, 995.
(22) Khan, G. F.; Ohwa, M.; Wernet, W. *Anal. Chem.* **1996**, *68*, 2939.
(23) Nguyen, A. L.; Luong, J. H. T. *Biosens. Bioelectron.* **1993**, *8*, 421.
(24) Kawagoe, J. L.; Niehaus, D. E.; Wightman, R. M. *Anal. Chem.* **1991**, *63*, 2961.
(25) Marzouk, S. A. M.; Cosofret, V. V.; Buck, R. P.; Yang, H.; Cascio, W. E.; Hassan, S. S. M. *Anal. Chem.* **1997**, *69*, 2646.
(26) Xin, Q.; Wightman, R. M. *Anal. Chim. Acta* **1997**, *341*, 43.
(27) Hill, B. S.; Scolari, C. A.; Wilson, G. S. *J. Electroanal. Chem.* **1988**, *252*, 125.
(28) Palmisano, F.; Centonze, D.; Malitesta, C.; Zambonin, P. G. *J. Electroanal. Chem.* **1995**, *381*, 235.
(29) Centonze, D.; Losito, I.; Malitesta, C.; Palmisano, F.; Zambonin, P. G. *J. Electroanal. Chem.* **1987**, *435*, 103.
(30) Khan, G. F. *Electroanalysis* **1997**, *9* (4), 325.
(31) Adams, R. N. *Electrochemistry at solid electrode*; Marcel Dekker Inc.: New York, 1969.
(32) Quinto, M.; Losito, I.; Palmisano, F.; Zambonin, C. G. *Fresenius J. Anal. Chem.* **2000**, *367*, 692.

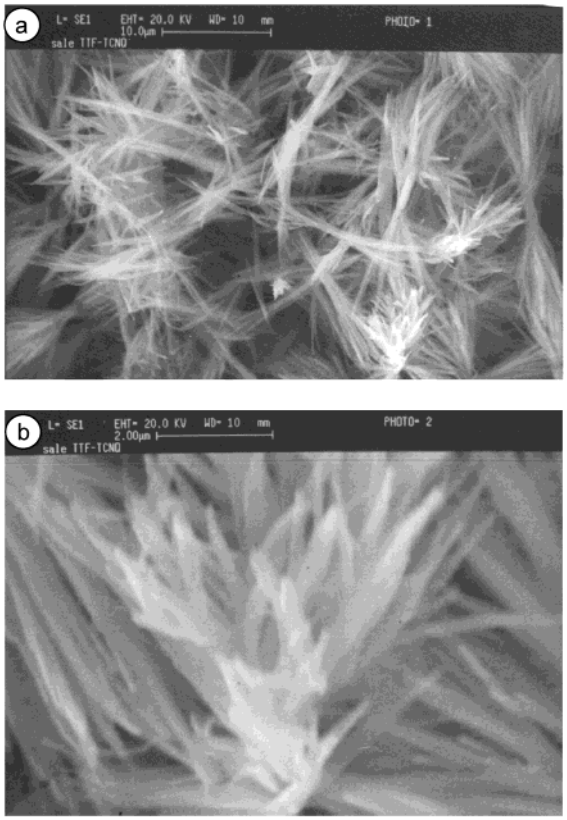

Figure 1. SEM photographs of the TTF−TCNQ crystals emerging from the $(PPy)_{ox}$ surface.

RESULTS AND DISCUSSION

The oxidation mechanism of flavoproteins at COS electrodes is still controversial and seems to depend on three main factors: the nature of the COS materials, electrode preparation, and applied potentials. In general, the oxidation mechanism can be ascribed to three different typologies: homogeneous mediation, direct transfer, and heterogeneous redox catalysis.[33] For example, some authors[16,34] suggested that the *N*-methylphenazinium (NMP)−TCNQ reacts with GOx after its dissolution, following a homogeneous catalysis. On the other hand, Albery et al.[17] proposed a mechanism in which enzyme oxidation takes place at the COS electrode surface by heterogeneous redox catalysis, while Hill et al.[27] suggested a cooperation between enzymes molecules in a different adsorption state at the COS surface: the strongly adsorbed enzyme (inactive) facilitates the electron transfer to the weakly (or reversibly) adsorbed enzyme. Freund and Brajter-Toth[35] suggested that the surface morphology could be responsible for the different electrochemical kinetics observed at TTF−TCNQ electrodes. In particular, if the COS orientation allows electron transmission perpendicularly to the electrode surface, direct electron transfer could be facilitated.[36]

Scanning electron microscopy (Figure 1a) of a $Pt/PPy_{ox}/TTF-TCNQ$ electrode can give an idea of the morphology of the TTF−TCNQ crystals emerging from the PPy_{ox} film. Polypyrrole is known to swell in the presence of organic solvents such as THF so that TCNQ can penetrate the film and TTF−TCNQ crystals can subsequently grow through the nonconducting film itself ensuring electrical contact with the underlying Pt layer. TTF−TCNQ crystals display a highly branched structure (anchored to the Pt electrode and maintained in place by the PPy film), the cross section of a typical branch being well below 1 μm (see Figure 1b). The final result is a highly roughened surface, with an effective area remarkably larger than the electrode geometric area. Covering such a surface with the enzyme solution causes GOx to fix (adsorb) onto the crystal surface; due to the high surface, a significant number of GOx molecules could even assume a proper orientation allowing direct electron transfer (vide infra) from the active site to TTF−TCNQ.

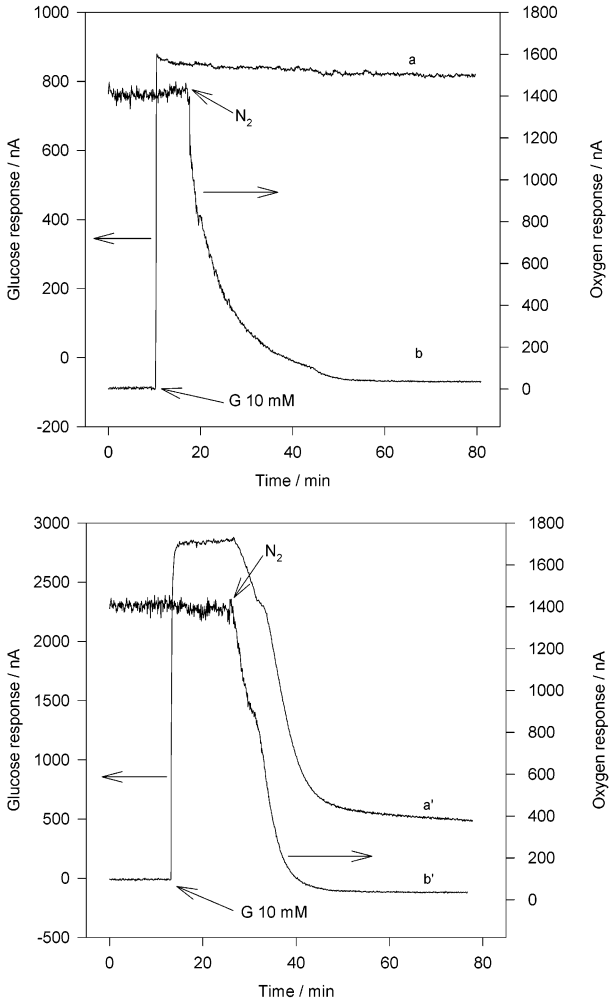

Figure 2. The 10 mM glucose response at a $Pt/(PPy)_{ox}/TTF-TCNQ/BSA-glut-GOx$ sensor polarized at +100 mV vs Ag/AgCl (curve a) and a $Pt/(PPy)_{ox}/BSA-glut-GOx$ sensor polarized at +700 mV vs Ag/AgCl (curve a′) as a function of the actual oxygen content (curves b and b′) measured by a Pt electrode polarized at −400 mV vs Ag/AgCl. Supporting electrolyte: stirred PBS buffer pH 7.0, I = 0.1 containing 10 mM Cl^-. The arrows indicate glucose addition or N_2 bubbling.

Figure 2 shows the different behavior of a $Pt/(PPy)_{ox}/TTF-TCNQ/BSA-glut-GOx$ sensor polarized at 100 mV (response a) and a $Pt/(PPy)_{ox}/BSA-glut-GOx$ sensor, polarized at 700 mV (response a′) as a function of the actual oxygen concentration measured by a second unmodified sensor chip (responses b and

(33) Albery, W. J.; Bartlett, P. N.; Cass, A. E. G. *Philos. Trans. R. Soc. London B* **1987**, *316*, 107.
(34) Kulys, J. J. *Biosensors* **1986**, *2*, 3.
(35) Freund, M. S.; Brajter-Toth, A. *Anal. Chem.* **1989**, *61*, 1048.
(36) Hillier, A. C.; Hossick Scott, J.; Ward, M. D. *Adv. Mater.* **1995**, *7* (4), 409.

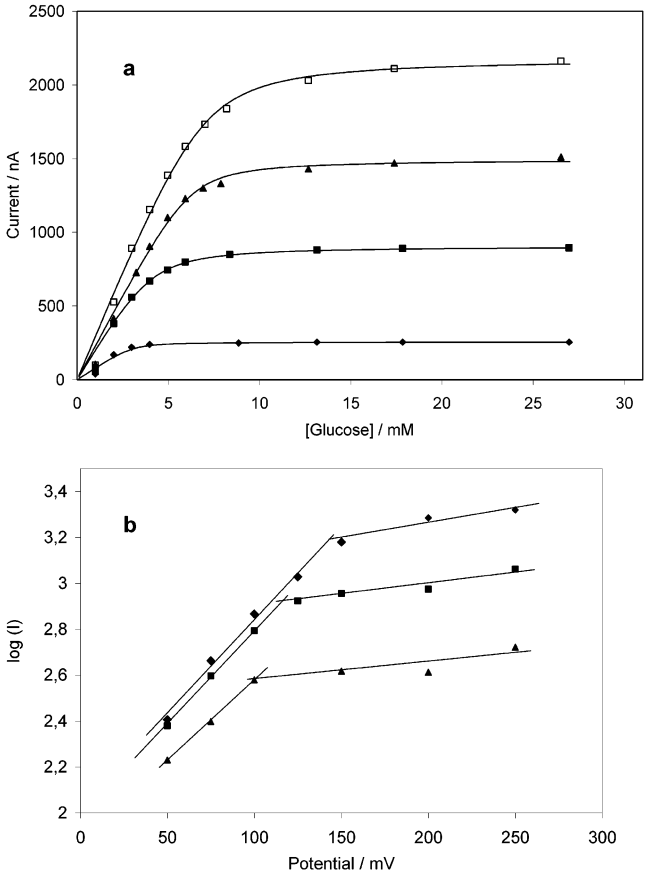

Figure 3. (a) Glucose calibration curves obtained at different applied potentials (●) 50, (■) 100, (▲) 150, and (□) 250 mV vs Ag/AgCl. Other conditions as in Figure 2. Solid lines are obtained by data fitting using eq 6 in the text. (b) Log *I* vs applied potential at different glucose concentrations for a Pt/$(PPy)_{ox}$/TTF−TCNQ/BSA−glut−GOx sensor: (◆) saturating glucose concentration (I_{max} calculated from a Lineweaver−Burk plot of data in Figure 2); 4 (■) and 2 mM (▲) glucose. Experimental conditions as Figure 2.

b′) connected to a second potentiostat. The arrows indicate glucose injection or N_2 bubbling to deoxygenate the solution. As can be seen, the 10 mM glucose response of the sensor modified with TTF−TCNQ is practically insensitive to the oxygen concentration, while the response of a COS-free sensor is dramatically reduced, but not totally suppressed, as would be expected. This could likely be due to an efficient recycling of residual O_2 traces within the film[37] rather than to a direct communication of GOx. Similar O_2 independence was observed at 5 mM glucose concentration, while a slight dependence was observed for glucose concentrations of ≤1 mM. Such an effect is quite common to all COS sensors and has been ascribed to oxygen competition, which is particularly effective especially at low glucose concentration.[38]

Figure 3a shows typical calibration plots obtained at different applied potentials in the stability region of the TTF−TCNQ salt; the solid lines are obtained by mathematical interpolation of experimental points by means of eq 6 (vide infra). Higher potentials lead to an increase in both linearity range and maximum current (I_{max}) as obtained by a Lineweaver−Burk plot of current−concentration data. A plot of log(I_{max}) versus applied potential is

(37) Bartlett, P. N.; Cooper, J. M. *J. Electroanal. Chem.* **1993**, *362*, 1.
(38) Martens, N.; Hindle, A.; Hall, E. A. H *Biosens. Bioelectron.* **1995**, *10*, 393.

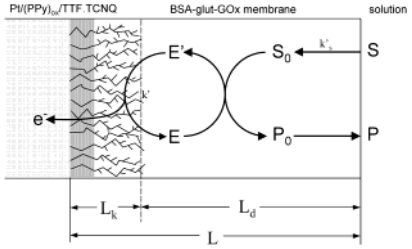

Figure 4. Schematic representation of processes involved in a Pt/$(PPy)_{ox}$/TTF−TCNQ/BSA−glut−GOx enzyme electrode. S, P: substrate and product, respectively. E, E′: oxidized and reduced form of the enzyme, respectively. For the meaning of other symbols, see text.

shown by the upper curve in Figure 3b. It is worth noting that a linear dependence is observed in a restricted potential range and that a deviation from linearity is observed at higher potentials. Interestingly, a transfer coefficient $\alpha = 0.47 \pm 0.3$ can be calculated from the slope of the linear part of the plot. It is worth noting that Albery et al.[33] demonstrated that α values of 0.5 and 0.25 should be observed for direct electron transfer and heterogeneous redox catalysis, respectively. Deviations from linearity observed at higher potentials can be reasonably ascribed to a change in the rate-determining step (rds); i.e., substrate mass transfer becomes slower than the electron transfer. This assumption is further supported by the evidence that the lower the substrate concentration the lower the potential where the change in the rds seems to occur (see the two lower curves in Figure 3b).

A simplified model accounting for substrate transport within the enzymatic membrane, enzyme kinetics, and enzyme reoxidation at TTF−TCNQ crystals has been devised (see Figure 4 for a schematic representation). The enzyme kinetics is assumed[39,40] to follow a Michaelis−Menten mechanism:

$$S + E \underset{k_{-1}}{\overset{k_1}{\rightleftharpoons}} SE^* \xrightarrow{k_{cat}} E' + P$$

where the Michaelis−Menten constant is $K_M = k_{-1}/(k_1 + k_{cat})$. The external diffusion resistance can usually be considered negligible compared with that of the membrane. Therefore, only the membrane-phase reactant diffusion is taken into consideration for the transport process in this model. To simplify the model, it is assumed that all the reactions, including enzyme catalysis, are confined and occur in a thin layer L_k immediately adjacent to the electrode surface and that L_k is separable from the effective membrane-phase diffusion layer L_d. A uniform substrate concentration (s_0) is assumed through the layer L_k.

In a steady-state situation, the total flux *j* (mol cm^{-2} s^{-1}) of this enzyme electrode system can be expressed as

$$j = k'_s[(s_\infty) - (s_0)] \quad (1)$$

$$= L_k[k_1(s_0)(e) - k_{-1}(se^*)] \quad (2)$$

$$= L_k[k_{cat}(se^*)] \quad (3)$$

$$= k'(e') \quad (4)$$

k' is the heterogeneous rate constant for enzyme reoxidation and k'_s is the mass-transfer rate constant given by $k'_s = D_m P/L$, where

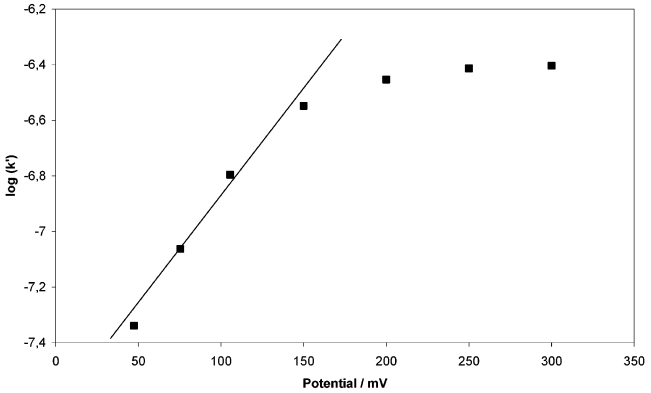

Figure 5. log k' vs applied potential. k' values are obtained from curve fittings of data in Figure 3a using eq 6 in the text.

D_m and P are the substrate diffusion and partition coefficients, respectively, in a membrane of thickness L.

The total concentration (e_∞) of the immobilized enzyme is given by

$$(e_\infty) = (e) + (se^*) + (e') \tag{5}$$

where (e) and (e') are the concentration of the oxidized and reduced forms, respectively, and (se^*) is the concentration of the enzyme−substrate complex.

Solving eqs 1−5 by elimination of the four unknowns (s_0), (e), (se^*), and (e'), it is possible to obtain the general expression for the flux:

$$j = \frac{\bar{e}_\infty k_{cat}}{1 + \frac{L_k k_{cat}}{k'} + \frac{K_M k_s'}{k_s' s_\infty - j}} \tag{6}$$

where ($\bar{e}_\infty$) (mol cm^{-2}) is the total amount of enzyme immobilized per unit area, i.e., ($\bar{e}_\infty$)= (e_∞)L_k.

Using the Levenberg−Marquardt algorithm, the experimental data shown in Figure 3a were fitted by eq 6 (see solid lines) by assuming[39] $K_M = 33$ mM and $k_{cat} = 175$ s^{-1}. The fitting procedure permits an estimation of the heterogeneous rate constant k' at the various applied potential values. A linear dependence of log k' from the applied potential should be expected.[41] Indeed, Figure 5 shows that such a linear dependence could be observed at least in a restricted potential range (0−150 mV), where electron transfer is assumed to be the rds. From the slope of the linear regression equation, a transfer coefficient of 0.47 ± 0.07 was found which is, again, in good agreement with the expected value ($\alpha = 0.5$).

A mass-transfer rate constant $k'_s = (2.8 \pm 0.4) \times 10^{-4}$ cm s^{-1} could be also estimated from the fitting procedure; assuming[42] a membrane thickness of ~10 μm, a value of 3×10^{-7} cm s^{-1} could be calculated for the D_mP product, which is quite reasonable considering the nature of the membrane (for instance, a D_mP of

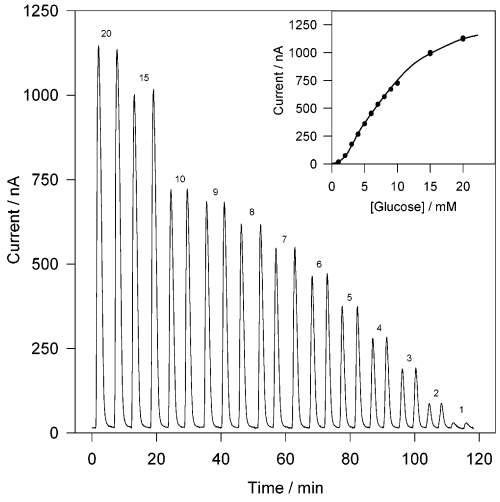

Figure 6. FIA peaks obtained at a Pt/(PPy)$_{ox}$/TTF−TCNQ/BSA−glut−GOx sensor for duplicate injections of glucose standards (1−20 mM, from right to left) and relevant calibration curve (inset). Carrier solution: phosphate buffer (I = 0.1, pH 7.0) containing 10 mM Cl$^-$. Applied potential: 100 mV vs Ag/AgCl, Flow rate: 100 μL/min. Injection volume: 110 μL.

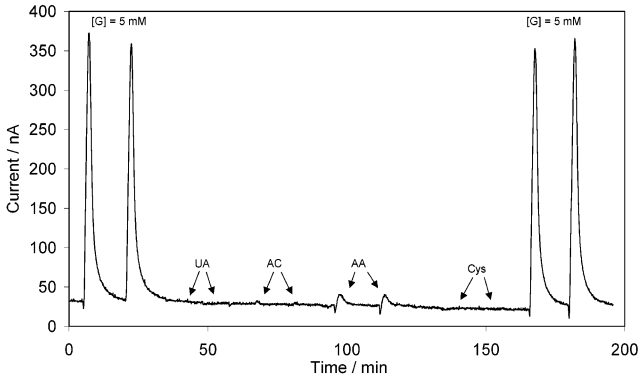

Figure 7. FIA peaks for duplicate injections of glucose standards (G, 5 mM), uric acid (UA, 0.5 mM), acetaminophen (AC, 0.2 mM), ascorbic acid (AA, 0.1 mM), and cysteine (Cys, 0.08 mM), for a Pt/(PPy)$_{ox}$/TTF−TCNQ/BSA−glut−GOx sensor; other conditions as in Figure 6.

2.4×10^{-6} cm^2 s^{-1} has been found for glucose in a poly(acrylamide) gel[43]). Response time, defined as the time necessary to achieve 95% of the steady-state current, was found to be ~5 s, which makes the sensor useful for flow injection analysis (FIA).

Figure 6 shows FIA responses of a typical disposable Pt/(PPy)$_{ox}$/TTF−TCNQ/BSA−glut−GOx sensor and the relevant calibration plot (see the inset), showing linearity up to 8 mM glucose and a remarkable sensitivity of 70 nA/mM. The influence of oxygen is more prominent al low glucose concentration and causes a decrease in the signal response. This effect has been already predicted by Martens and Hall[40] for membranes thicker than 0.4 μm.

Electroactive species amenable to be electrocatalytically oxidized by TTF−TCNQ salt could potentially produce a glucose bias. The sensor response to the most common interferences (ascorbate, urate, cysteine, paracetamol) at their physiological concentrations is shown in Figure 7. As can be seen urate, acetaminophen and cysteine gave undetectable signals; 0.1 mM ascorbate

(39) Swoboda, B. E. P.; Massey, V. *J. Biol. Chem.* **1965**, *240*, 2209.
(40) Martens, N.; Hall, E. A. H. *Anal. Chem.* **1994**, *66*, 2763.
(41) Bard, A. J.; Faulkner, L. R. In *Electrochemical Methods;* Bard, A. J., Ed.; Wiley and Sons: New York, 2000; Vol. II.
(42) Guerrieri, A.; De Benedetto, G. E.; Palmisano, F.; Zambonin, P. G. *Analyst* **1995**, *120*, 2731.
(43) Gorton, L. *Anal. Chim. Acta* **1985**, *178*, 247.

produced a response ~3.1 ± 1.4% that of 5 mM glucose, as measured over a three-week period of sensor operation. The low AA interference level observed results from an effective rejection of electroactive substances rather than from a very high glucose/AA sensitivity ratio as, for instance, reported by Khan et al.[22] (observed current density for 0.1 mM AA equal to 130 $\mu A/cm^2$). In the present case, due to the presence of an overoxidized PPy membrane, AA can only be oxidized at the TTF−TCNQ free surface. The low value of AA oxidation current (3.5 $\mu A/cm^2$ for 0.1 mM AA) reinforces the assumption (vide ante) of a very high coverage of exposed TTF−TCNQ by GOx, which should be responsible for the direct electrochemistry of the enzyme.

CONCLUSIONS

A disposable, reagentless, third-generation glucose biosensor has been obtained that is essentially oxygen- and interference-free. This has been made possible due to a peculiar in situ synthesis of TTF−TCNQ onto an anti-interference layer of nonconducting poly(pyrrole) film. The final device is also mechanically stable and can be easily incorporated in a flow-through cell. The devised procedure has the potential to be adapted to mass-scale production.

ACKNOWLEDGMENT

Work performed with financial support from CNR target project "Biotechnology". Prof. M. A. Del Nobile is gratefully acknowledged for his help in data fittings.

Received for review June 13, 2002. Accepted September 27, 2002.

AC0258608